



Extraction of nickel ions using nanoporous adsorbent material from waste glass

Z. Karm^{a*} • S. A. Ajeel^a • B. A. Abdulhussein^b

^aDepartment of Production Engineering and Metallurgy, University of Technology, Baghdad, Iraq

^bDepartment of Chemical Engineering, University of Technology, Baghdad, Iraq

Received 01 06 2024; accepted 06 06 2024

Available 10 31 2024

Abstract: This study aims to create a porous glass adsorbent from waste glass to extraction nickel ions from its aqueous solution. The process involves converting waste glass to porous glass using 1:1:1:1 lime, sodium chloride, and sodium bicarbonate, followed by reacting with waste glass at 800 °C. The porous glass surface morphology, elemental composition, and functional groups were analyzed using SEM, EDS, and FT-IR techniques. The outcome parameters used in this study are adsorbent dosage (10 g), contact time (150 min), heavy metal ion concentration (100 mg/l), and pH of 6. The adsorption capacity resulting from these parameters is 9.28 mg/g using the porous extract adsorbent for the extraction of nickel ions from its solutions. According to the findings. The proportion extraction of nickel ions increased directly with an increase in the adsorbent dosage, nickel ion concentration, contacting time, and pH. In addition, the Langmuir isotherm ($R^2 = 0.98, K_L=0.072$) has shown better performance than the Freundlich adsorption isotherm ($R^2 = 0.93, N=1.598$) for the adsorption of the Ni(II) in this study.

Keywords: Extraction, porous glass, adsorption isotherms, Ni(II) Ions

*Corresponding author.

E-mail address: zamen.K.mekhelf@uotechnology.edu.iq (Z. Karm).

Peer Review under the responsibility of Universidad Nacional Autónoma de México.

1. Introduction

Two-thirds of the chemical elements that occur naturally on Earth are called minerals, and due to their special qualities, they are widely used in many different industries, such as building, energy, technology, and transportation. (Alvial-Hein et al., 2021). Compared to most non-renewable resources, minerals have greater capacity and potential for sustainable economic activities. With increasing progress in science and technology, it has led to increased consumption of metals in current environments. As a result, after the metal has been manufactured and reached the end of its usefulness, natural resources are depleted and enormous amounts of waste are produced, causing economic losses and environmental issues (Abu-Daabes et al., 2023; He et al., 2020; Jiang et al., 2006). Among these important metals, nickel is considered the most significant strategic resource and is distinguished by its small reserves (Alvial-Hein et al., 2021; He et al., 2020).

Owing to the depletion of nickel resources and tightening of environmental protection requirements, many conventional nickel mines are anticipated to close during the next few decades (Abu-Daabes et al., 2023; He et al., 2020). One solution to these problems is to expand the recycling of secondary resources before the depletion of nickel resources (Jiang et al., 2006). Among the secondary resources of nickel, nickel electroplating effluent has substantial value for exploitation and is used as a secondary resource based on the principles of sustainable development (Gao et al., 2023). In addition, nickel is found in drinking water because it is present in alloys used in chrome-plated or nickel-plated faucets that come into contact with drinking water (Al-Amrani et al., 2023). Additionally, the dissolution of naturally Ni-bearing strata in groundwater is a common cause of the presence of Ni in water sources (Mahiya et al., 2014). According to Hasan et al. (2012) the maximum allowable limit of Ni(II) in water is 0.02 mg L⁻¹. When nickel levels are too high, they have harmful effects on people. Additionally, according to Borba et al. (2006) aspiration of nickel and its compounds may result in serious health issues, such as nasopharynx, lung, and kidney problems, gastrointestinal distress, pulmonary fibrosis, dermatological illnesses, and aggressive cancers.

Therefore, it is necessary to extract nickel from these aqueous media. There are many methods for extracting nickel ions, including liquid-liquid extraction, ion exchange, co-precipitation, and solid-phase extraction (SPE), which is one of the methods used to separate and concentrate nickel. (Coman et al., 2013; Li et al., 2022; Meshram et al., 2018). Due to the advantages of the SPE method, which include the use of sorbents that are cost-effective and ensure safety for hazardous samples, the SPE method has been widely used for preconcentration and separation of metals. (Sivrikaya et al., 2014).

Several absorbents are commonly used, including silica gel, A. Barbadensis Miller waste leaf powder, natural bentonite, activated carbon, zeolite, vermiculite, and porous glass (Gawhane, 2014; Gupta & Kumar, 2019; Hussain et al., 2020; Islam et al., 2019; Samad et al., 2022; Šuránek et al., 2021; Malamis & Katsou, 2023). Although many studies have been conducted in the last ten years on solid-phase extraction, the search for better sorbents has persisted. Among these materials, porous glass has received considerable attention. This study prepared porous adsorbent materials by processing glass waste into adsorbent materials for the extraction of Ni(II) ions. The major factors influencing the adsorption process were also examined, including pH, adsorbent dosage, initial metal ion concentration, and contact time. To explain the competitive behavior of the studied metal ions, Langmuir and Freundlich models were applied.

2. Materials and methods

2.1. Chemicals and methods of analysis

All chemicals used in this study are of analytical grade. The chemicals (lime, sodium chloride, and sodium bicarbonate) as well as hydrochloric acid and sodium hydroxide to adjust the pH were provided by Sigma-Aldrich.

The primary functional groups present in the porous extract adsorbents were investigated using Fourier transform infrared spectroscopy (FTIR-4200, JASCO, Hachioji, Tokyo, Japan). By using scanning electron microscopy and energy-dispersive spectrometry (SEM 6000-EDS2300, JEOL, Akishima, Tokyo, Japan), surface morphology and elemental distribution were observed.

2.2. Preparation of non-glass porous materials

The transparent white glass waste was treated with boiling water to ensure cleanliness. After cleaning and washing, the waste glass was kiln-dried and grinded into a fine powder using a dedicated cutter mill. The grinding conditions (15 min, 350 rpm, ball characteristics: 25 mm stainless steel balls) were followed by sieving through a sieve less than a 25-micrometer size. A 1:1:1:1 ratio of powder glass interacted with lime, sodium chloride, and sodium bicarbonate, respectively, and the mixture was placed in a furnace at 800 °C for 1 h to produce a highly porous and non-vitreous adsorbent. It should be noted that all raw materials melt at temperatures below 800 °C. Lime may have served as a flux during the reaction, whereas sodium chloride and sodium bicarbonate were meant to make the final product porous and non-vitreous. Lime may also function as a solid foundation, which helps the glass react more easily with other elements (Ofomaja & Ho, 2007; Cruz-Lopes et al., 2021).

2.3. Batch adsorption studies

The adsorption experiments were conducted in Erlenmeyer flasks (150 ml capacity). Various contact periods (50–250 min), pH levels (2–10), adsorbent dosages (2–10 g), and initial nickel ion concentrations (40–140 ppm) were used to study the adsorption of Ni(II) using the porous glass adsorbent.

The adsorbent was added to a solution of known volume, metal ion concentration, and pH at room temperature. Whatman pore-size filtration membrane filter paper (0.45 μm) was used to separate the adsorbent from the Ni(II) solution. A flame atomic absorption spectrophotometer was used to measure the Ni(II) concentration before and after adsorption, after which the sample was extracted. Using (Equation 1) (Si et al., 2022) the adsorption capacity q_e is derived.

$$q_e = \frac{(C_o - C_e)v}{w} \quad (1)$$

3. Results and dissection

3.1. Characterization of the porous glass adsorbent

To evaluate the vibration frequency of the functional groups in the adsorbent responsible for adsorption, a porous glass adsorbent was detected by FTIR analysis of the presence of several distinct functional groups, as shown in (Figure 1). Also, Table 1 provides an analysis of the wave number and appearance of broad and functional groups derived from the absorption spectra. 3465.05 cm^{-1} , 1575.49 cm^{-1} , and 1417.49 cm^{-1} were 515.06 cm^{-1} suggests that NaCl was used as both an adsorbent and reactant, demonstrating the significance of NaCl in the structural and chemical reactions of glass with porous adsorbent. According to the above results, there are many oxygen-containing functional groups on the surface of the adsorbent materials, and these functional groups can offer many active sites for the removal of Ni(II). In addition to revealing the chemically reactive functional groups (-OH) that enhance the adsorption of heavy metal ions (Si et al., 2022).

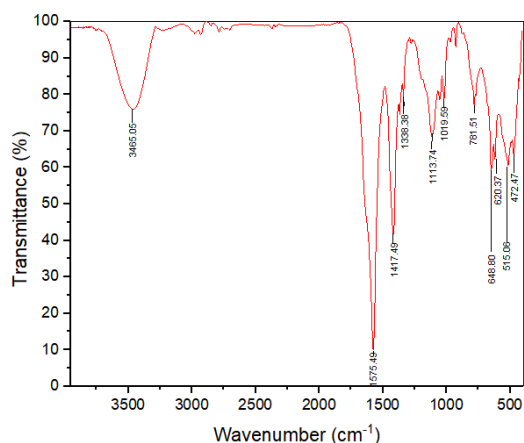


Figure 1. FTIR spectrum of porous glass adsorbent.

Table 1. FTIR analysis of the functional groups for porous glass adsorbent.

Spectrum No.	Wave number cm^{-1}	Appearance of broad	Functional group assignment
1	3465.05	strong	O-H stretching vibration
2	1575.49	strong	C=C stretching
3	1417.49	strong	O-H bending
4	1338.38	medium	O-H bending
5	1113.74	medium	C=C stretching vibration
6	1019.59	medium	C-H bending
7	781.51	medium	C-H bending
8	648.80	medium	C-H wagging vibration
9	620.37	medium	C-H bend
10	515.06	strong	C-Br stretching vibration
11	472.47	strong	C-I stretching vibration

Figure 2 shows SEM micrographs of the porous glass adsorbent. Figure 2 shows that porous glass is present in diverse sizes as beads, flakes, ovals, and granule-shaped beads. Also, Figure 2 shows the availability of multiple cavities and holes that allow for the adsorption of Ni(II) ions. In addition, the surface of the porous glass adsorbent was highly irregular, allowing for the adsorption of Ni(II) ions.

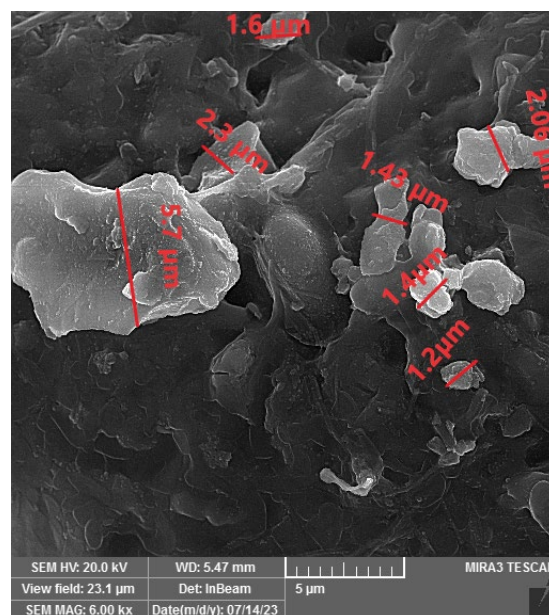


Figure 2. SEM of the porous extract adsorbent.

Figure 3 and Table 2 show the EDX spectra of the porous glass adsorbent. The spectra demonstrates that a sizable

portion of the porous material included carbon, oxygen, sodium, calcium, magnesium, aluminum, chlorine, and silica. While the presence of a small amount of sulfur is indicative of its presence in waste glass, after adsorption of the nickel ions, as shown in Figure 4 and Table 2, we noticed a decrease in the carbon and oxygen content, as seen in the obtained spectrum (Figure 4). These findings showed that O and C were the predominant elements, assuming that they were the surface sites for adsorbing Ni(II) ions. According to those findings, O offered many hydroxyl adsorption sites for adsorbing Ni(II) ions. Additionally, Figure 4 shows that the Ca peak is absent, with the remaining elements' peaks remaining but diminished. In addition, the adsorbed Ni(II) ions caused the appearance of a new peak.

The functional group results, which had previously been validated by the FTIR results, complemented the EDS results by verifying the presence of these components inside the functional groups.

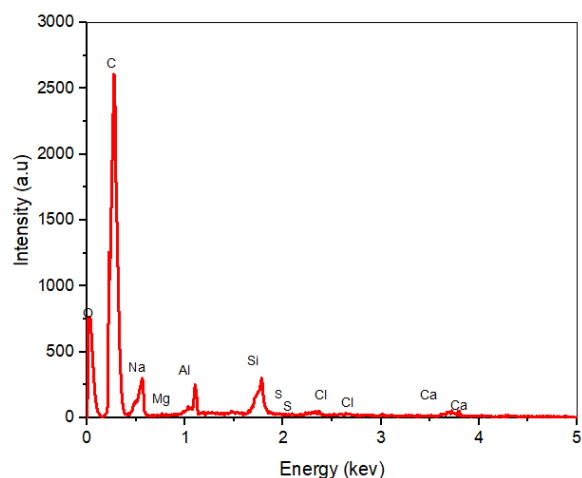


Figure 3. EDX spectra of the porous extract adsorbent.

Table 2. EDX analysis of the adsorbent porous extract before and after adsorption.

Elt	W% before adsorption	W% after adsorption
C	82.77	74.91
O	13.02	7.54
Na	0.68	5.89
Mg	0.28	0.18
Al	0.29	0.24
Si	1.64	0.85
S	0.41	0.31
Cl	0.22	0.11
Ca	0.69	--
Ni	--	9.97
Total	100	100

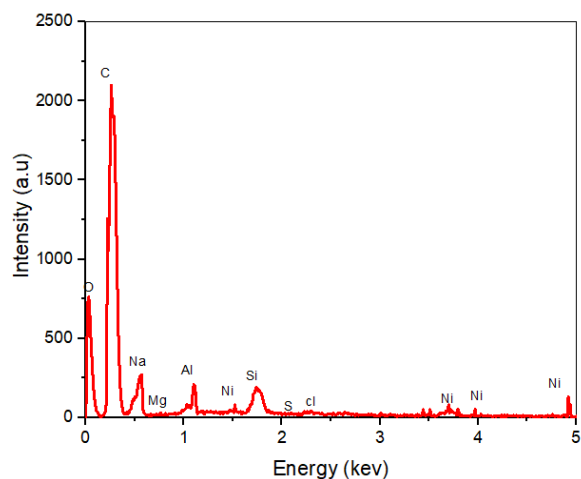


Figure 4. EDX spectra of the porous extract adsorbent after adsorption.

3.2. Factors affecting adsorption

This study used different shaking times (50–250 min) with a dose of adsorbent of 15 g/L, a concentration of Ni(II) of 100 mg/l, and a pH of the solution set at 3 to understand how the contact time affects the adsorption of Ni(II) using a porous glass adsorbent and determine the ideal contact elapsed period between the adsorbent and adsorbate.

Figure 5 shows the outcome of the contact time impact with adsorbent capacity (q_e) in mg/g, which indicates that an increase in interaction duration is accompanied by a q_e increase up to 40 min into the initial period and there was very quick adsorption followed by a gradual increase in the adsorption rate. The process of adsorption reached equilibrium at an adsorbent capacity of 9.285 mg/g at 150 min. After 150 minutes, no discernible difference in Ni(II) elimination was seen. The findings showed that both the contact duration and the adsorption capacity increased and eventually decreased as the contact time increased. This occurred because at the beginning of the contact time, there were more empty binding sites available for metal adsorption; however, as the contact time increased, these binding sites gradually became saturated by the metal ions. It is difficult for metal ions to fill the remaining vacant surface binding sites; this explains the decrease in the capacity of adsorption after 150 min (Gulipalli et al., 2011) because of the repulsive interactions between the metal ions in the adsorbent sites and those in the bulk liquid phase. In addition, one of the factors influencing the uptake of heavy metals from aqueous solutions is the pH of the solution.

The pH has a substantial impact on the process because it affects the functionality groups and may cap the sorption rates (Esmaeili & Beni, 2018). pH is one of the most crucial factors in the adsorption process because it can affect the properties of the metal in solution and the loading of active sites on the

surface. According to Ofomaja and Ho (2007) assert that several reactions involving heavy metal ions are influenced by the pH of an aqueous solution, including dissociation, hydrolysis, complexation, and precipitation. The availability and speciation of ions are also impacted by pH, which has an impact on adsorption capacity. The examination into the extraction of Ni(II) indicated these adsorbents' Ni(II) adsorption capacities at various pH ranges between 2.0 and 10.0, 150 min of shaking, 15 g/L of adsorbent dose, and 100 mg/l of Ni(II) concentration, as shown in (Figure 6).

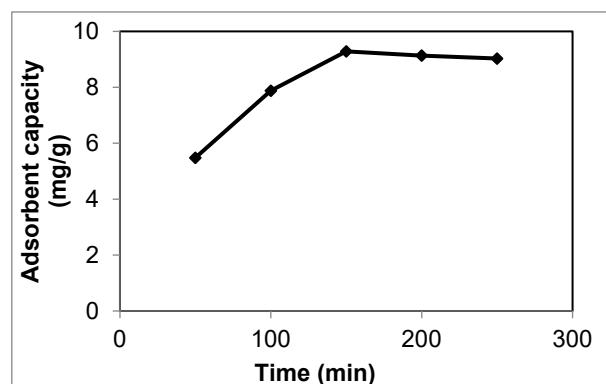


Figure 5. Effect of contact duration on the adsorbent capacity of Ni(II).

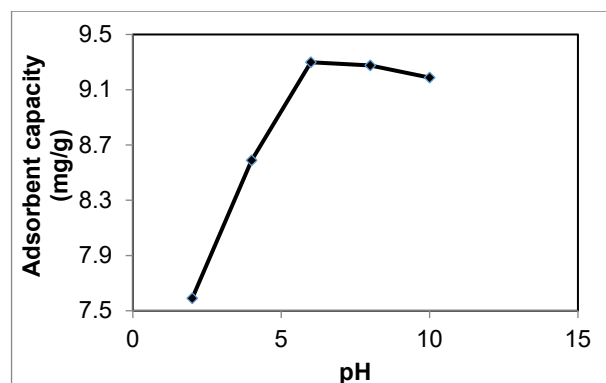


Figure 6. Effect of pH on the adsorbent capacity of Ni(II).

Hence, the adsorption capacity of porous glass adsorbent for Ni(II) is lower at acidic pH than alkaline pH where the hydroxyl groups of the adsorbent can be destroyed at acidic pH. Whereas the adsorbent surface became more negatively charged as the pH increased, causing a dramatic increase in Ni(II) adsorption, followed by a minor drop. Ni(II) ions, such as Ni(OH)₂, precipitate simultaneously at pH levels greater than 7.0, which may lead to misinterpretation of the adsorption properties (Cruz-Lopes et al., 2021).

At pH 6.0, porous glass adsorbent maximum Ni(II) adsorbent capacity of 9.28 mg/g was observed. The impact of different adsorbent dosages (2 to 10 g) on the extraction of

Ni(II) ions from aqueous solutions at a pH of 6, shaking times of 150 min, and a concentration of Ni(II) of 100 mg/l is shown in (Figure 7). According to the findings, Ni(II) ion adsorption rises from 20.9 mg/g at lower adsorbent doses (2 g) to 9.28 mg/g at higher adsorbent doses (10 g). This can be explained by the fact that adsorption is lower at low doses because the initial concentration is constant when different doses are used.

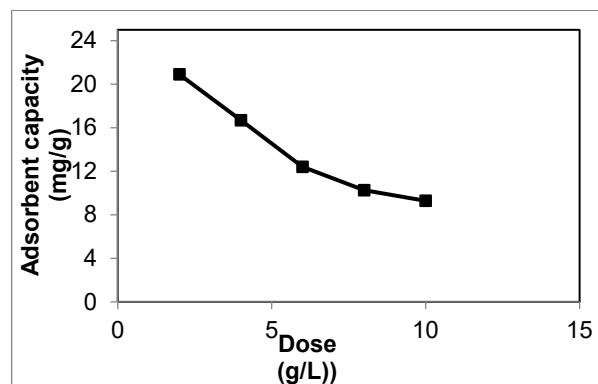


Figure 7. Effect of dose of adsorbent on the adsorbent capacity of Ni(II).

The effect of different concentration of Ni(II) of (40-140 mg/l), shaking times of 150 min, dose of adsorbent of 10 g/L, and the pH of 6 is shown in (Figure 8). According to the results of the initial adsorbate concentration (Figure 8), the adsorption capacity increased as the adsorbate concentration increased from 40 mg/L to 140 mg/L. Ni(II) ions adsorption rises from 3.87 mg/g at 40 mg concentration of Ni(II) to 13.03 mg/g at 140 mg/l of concentration Ni(II).

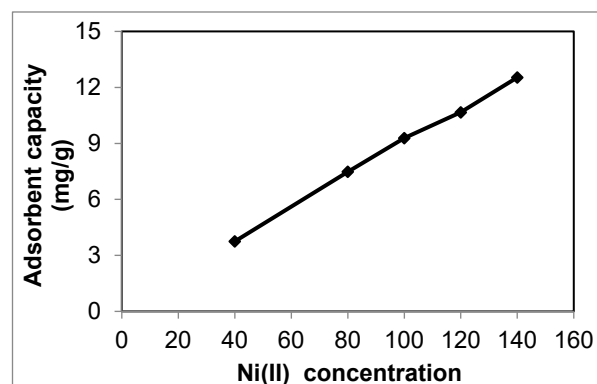


Figure 8. Effect of adsorbate concentration on the adsorbent capacity of Ni(II).

The metal ions can easily occupy the available binding sites on the adsorbent surface at lower adsorbate concentrations when there are fewer adsorbate ions. However, at higher adsorbate concentrations, the binding sites become saturated by the metal ions, and the active sorbent site is not

able to accommodate more Ni(II) ions, leading to less metal adsorption (Coman et al., 2013; Gawhane, 2014; Gupta & Kumar, 2019; Islam et al., 2019; Li et al., 2022; Malamis & Katsou, 2023; Sivrikaya et al., 2014; Šuránek et al., 2021).

Langmuir and Freundlich isotherms were used in this investigation. The relationship between the amount of metal ions adsorbed and the equilibrium concentration in solution is often established using these isotherms. Langmuir adsorption isotherm refers to the monolayer coverage of the adsorbent, while the Freundlich isotherm model, denotes surface heterogeneity and exponential distribution of active sites and their energies (Nandiyanto et al., 2023; Prabhu et al., 2023).

To assist in offering the mechanism of the adsorption process. Figure 6 and Figure 7 show the Langmuir and Freundlich isotherms, respectively, for the Ni(II) ions adsorption using the Langmuir (Equation 2) (Huang et al., 1991)

$$\frac{1}{q_e} = \frac{1}{q_m} + \frac{1}{q_m K_L} \cdot \frac{1}{C_e} \quad (2)$$

(Equation 3) represents the Freundlich equations (Huang et al., 1991).

$$q_e = K_f C_e^n \quad (3)$$

Figure 9, Figure 10 and Table 3 show the Langmuir and Freundlich models, respectively, for Ni(II) ions on a porous glass adsorbent. As shown in Table 2, the data in this investigation were well fitted to the Langmuir model (R2 = 0.98), indicating that metal ion sorption was primarily conducted as a monolayer on the porous glass adsorbent surface.

The Langmuir isotherm model yielded qmax and kL values for Ni(II) ions of 25.12 mg g⁻¹ and 0.072 Lmg⁻¹, respectively. A high kL value indicates a high affinity between the porous glass adsorbent surface and Ni(II) ions, and the qmax value points out the maximum adsorption capacity when the surface of the sorbent is entirely covered by metal ions. KF was proportional to the adsorption capacity, and N constants with respect to adsorption intensity. KF and N of the Freundlich model had values of 23.73 L g⁻¹ and 1.598 respectively, which represents a relative estimate of the adsorption capacity. Thus, from the isotherm results, the Langmuir model accurately fitted the experimental data.

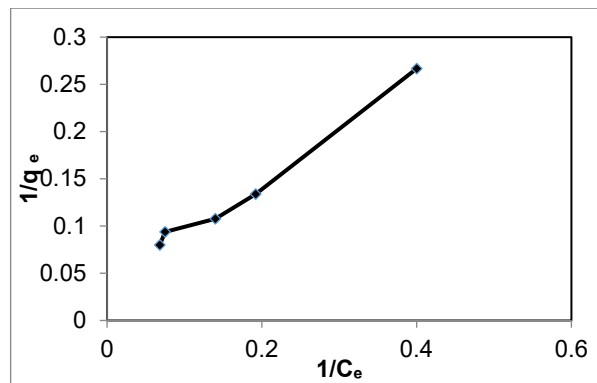


Figure 9. Isotherm of the Langmuir adsorption model of Ni(II) ions.

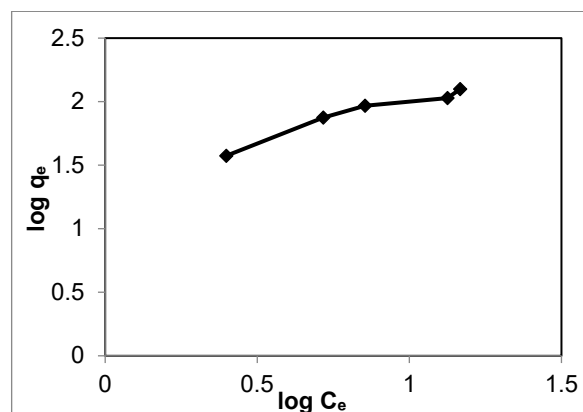


Figure 10. Isotherm of Freundlich's adsorption model of Ni(II) ions.

Table 3. Parameters of the Langmuir and Freundlich isotherm model.

Langmuir			Freundlich		
q _m mg. g ⁻¹	K _L	R ²	K _F	N	R ²
25.12	0.072	0.98	23.73	1.598	0.93

4. Conclusions

A porous glass adsorbent has been created in this study. According to FTIR, SEM, and EDX investigations. FTIR results show that there are many functional groups on the surface of the adsorbent materials, and these functional groups offer many active sites for the extraction of Ni(II). SEM results showed that the adsorption materials had a porous surface, which undoubtedly contributed to the effective adsorption. In addition, EDS validated the FTIR results, confirming the presence of oxygen, sodium, calcium, potassium, chlorine, and silica in the adsorbent.

This study examined the impact of contact time, pH, initial Ni(II) ion content, and adsorbent dose on the absorption capacity. The obtained results showed that pH 6, contact period of 150 min, and adsorbent dose of 10 g at room temperature are the optimum parameters for the extraction of Ni(II) ions, which resulted in almost 9.2 mg/g of adsorption capacity utilizing porous glass adsorbent. The Langmuir isotherm model provides a satisfactory correlation between the equilibrium data. The correlation coefficient of the Langmuir model was approximately 0.98. Moreover, these coefficients were greater than 0.93 in the Freundlich model. These findings suggest that the use of porous glass as an adsorbent for removing Ni(II) ions from aqueous solutions is a cost-effective and efficient way to protect the environment and reduce water pollution.

Conflict of interest

The authors have no conflict of interest to declare. The authors have no conflicts of interest of any kind.

Acknowledgements

The authors very thank to Department of Production Engineering and Metallurgy, University of Technology, Baghdad, Iraq for assisting in completing this work.

Funding

The authors received no specific funding for this work.

References

- Abu-Daabes, M. A., Abu Zeitoun, E., & Mazi, W. (2023). Competitive adsorption of quaternary metal ions, Ni²⁺, Mn²⁺, Cr⁶⁺, and Cd²⁺, on acid-treated activated carbon. *Water*, 15(6), 1070. <https://doi.org/10.3390/w15061070>
- Al-Amrani, W. A., Abdullah, R., Megat Hanafiah, M. A. K., & Suah, F. B. M. (2023). Removal of Ni (II) Ions by Citric Acid-Functionalised Aloe vera Leaf Powder-Characterisation, Kinetics, and Isotherm Studies. *Journal of Ecological Engineering*, 24(4), 217-227.
- Alvial-Hein, G., Mahandra, H., & Ghahreman, A. (2021). Separation and recovery of cobalt and nickel from end of life products via solvent extraction technique: A review. *Journal of Cleaner Production*, 297, 126592. <https://doi.org/10.1016/j.jclepro.2021.126592>
- Borba, C. E., Guirardello, R., Silva, E. A., Veit, M. T., & Tavares, C. R. G. (2006). Removal of nickel (II) ions from aqueous solution by biosorption in a fixed bed column: experimental and theoretical breakthrough curves. *Biochemical Engineering Journal*, 30(2), 184-191. <https://doi.org/10.1016/j.bej.2006.04.001>
- Coman, V., Robotin, B., & Ilea, P. (2013). Nickel recovery/removal from industrial wastes: A review. *Resources, Conservation and Recycling*, 73, 229-238. <https://doi.org/10.1016/j.resconrec.2013.01.019>
- Cruz-Lopes, L. P., Macena, M., Esteves, B., & Guiné, R. P. (2021). Ideal pH for the adsorption of metal ions Cr⁶⁺, Ni²⁺, Pb²⁺ in aqueous solution with different adsorbent materials. *Open Agriculture*, 6(1), 115-123. <https://doi.org/10.1515/opag-2021-0225>
- Esmaeili, A., & Aghababai Beni, A. (2018). Optimization and design of a continuous biosorption process using brown algae and chitosan/PVA nano-fiber membrane for removal of nickel by a new biosorbent. *International Journal of Environmental Science and Technology*, 15, 765-778. <https://doi.org/10.1007/s13762-017-1409-9>
- Gao, W., He, W., Zhang, J., Chen, Y., Zhang, Z., Yang, Y., & He, Z. (2023). Effects of biochar-based materials on nickel adsorption and bioavailability in soil. *Scientific Reports*, 13(1), 5880. <https://doi.org/10.1038/s41598-023-32502-x>
- Gawhane, S. (2014). Scavenging of Nickel(II) from Aqueous Wastes by Adsorption with Granular Activated Carbon (GAC). In *Applied Mechanics and Materials* (Vol. 612, pp. 187-192). Trans Tech Publications, Ltd. <https://doi.org/10.4028/www.scientific.net/AMM.612.187>
- Gulipalli, C. S., Prasad, B., & Wasewar, K. L. (2011). Batch study, equilibrium and kinetics of adsorption of selenium using rice husk ash (RHA). *Journal of Engineering Science and Technology*, 6(5), 586-605. <https://doaj.org/article/e1aba5929b6749e58618d8c001c7ef0f>
- Gupta, S., & Kumar, A. (2019). Removal of nickel (II) from aqueous solution by biosorption on A. barbadensis Miller waste leaves powder. *Applied Water Science*, 9, 1-11. <https://doi.org/10.1007/s13201-019-0973-1>
- Hasan, Z., Anwar, Z., Khattak, K. U., Islam, M., Khan, R. U., & Khattak, J. Z. K. (2012). Civic pollution and its effect on water quality of river Toi at district Kohat, NWFP. *Research Journal of Environmental and Earth Sciences*, 4(3), 334-339.

- He, D., Zeng, L., Zhang, G., Guan, W., Cao, Z., Li, Q., & Wu, S. (2020). Extraction behavior and mechanism of nickel in chloride solution using a cleaner extractant. *Journal of Cleaner Production*, 242, 118517.
<https://doi.org/10.1016/j.jclepro.2019.118517>
- Huang, C., Huang, C. P., & Morehart, A. L. (1991). Proton competition in Cu(II) adsorption by fungal mycelia. *Water Research*, 25(11), 1365–1375.
[https://doi.org/10.1016/0043-1354\(91\)90115-7](https://doi.org/10.1016/0043-1354(91)90115-7)
- Hussain, Z., Sultan, N., Ali, M., Naz, M. Y., AbdEl-Salam, N. M., & Ibrahim, K. A. (2020). Thermochemical conversion of waste glass and mollusk shells into an absorbent material for separation of direct blue 15 azo dye from industrial wastewater. *ACS omega*, 5(29), 18114-18122.
<https://doi.org/10.1021/acsomega.0c01680>
- Islam, M. A., Awual, M. R., & Angove, M. J. (2019). A review on nickel (II) adsorption in single and binary component systems and future path. *Journal of Environmental Chemical Engineering*, 7(5), 103305.
<https://doi.org/10.1016/j.jece.2019.103305>
- Jiang, N., Chang, X., Zheng, H., He, Q., & Hu, Z. (2006). Selective solid-phase extraction of nickel (II) using a surface-imprinted silica gel sorbent. *Analytica Chimica Acta*, 577(2), 225-231.
<https://doi.org/10.1016/j.aca.2006.06.049>
- Mahiya, S., Lofrano, G., & Sharma, S. K. (2014). Heavy metals in water, their adverse health effects and biosorptive removal: A review. *International Journal of Chemistry*, 3(1), 132-149.
- Malamis, S., & Katsou, E. (2013). A review on zinc and nickel adsorption on natural and modified zeolite, bentonite and vermiculite: Examination of process parameters, kinetics and isotherms. *Journal of Hazardous Materials*, 252, 428-461.
<https://doi.org/10.1016/j.jhazmat.2013.03.024>
- Meshram, P., Abhilash, B., & Pandey, D. (2018). Advanced Review on extraction of nickel from primary and secondary sources. *Mineral Processing and Extractive Metallurgy Review*, 40(3), 157–193.
<https://doi.org/10.1080/08827508.2018.1514300>
- Nandiyanto, A. B. D., Ragadhita, R., Fiandini, M., & Maryanti, R. (2023). Curcumin dye adsorption in aqueous solution by carbon-based date palm seed: Preparation, characterization, and isotherm adsorption. *Journal of Applied Research and Technology*, 21(5), 808-824.
<https://doi.org/10.22201/icat.24486736e.2023.21.5.1972>
- Ofomaja, A. E., & Ho, Y. S. (2007). Effect of pH on cadmium biosorption by coconut copra meal. *Journal of Hazardous Materials*, 139(2), 356-362.
<https://doi.org/10.1016/j.jhazmat.2006.06.039>
- Prabhu, N., Shetty, P., Kumari, P., & Kagatkar, S. (2023). Inhibitive action of 2-aminobezothiazole on the deterioration of AA6061-SiC composite in 0.5 M HCl medium: Experimental and theoretical analysis. *Journal of Applied Research and Technology*, 21(4), 581-597.
<https://doi.org/10.22201/icat.24486736e.2023.21.4.1953>
- Samad, S. A., Arafat, A., Ferrari, R., Gomes, R. L., Lester, E., & Ahmed, I. (2022). Adsorption studies and effect of heat treatment on porous glass microspheres. *International Journal of Applied Glass Science*, 13(1), 63-81.
<https://doi.org/10.1111/ijag.16352>
- Si, R., Pu, J., Luo, H., Wu, C., & Duan, G. (2022). Nanocellulose-based adsorbents for heavy metal ion. *Polymers*, 14(24), 5479.
<https://doi.org/10.3390/polym14245479>
- Sivrikaya, S., İmamoğlu, M., & Kara, D. (2014). On-line solid phase extraction of nickel, copper, and cadmium using a newly synthesized polyamine silica gel-loaded mini-column for flame atomic absorption spectrometric determination. *Atomic Spectroscopy*. 35(4), 168–176.
<https://doi.org/10.46770/AS.2014.04.005>
- Šuránek, M., Melichová, Z., Kureková, V., Kljajević, L., & Nenadović, S. (2021). Removal of nickel from aqueous solutions by natural bentonites from slovakia. *Materials*, 14(2), 282.
<https://doi.org/10.3390/ma14020282>
- Li, T., Bian, H., Wang, W., Fan, X., Tao, L., Yu, G., & Deng, S. (2022). Removal of low-concentration nickel in electroplating wastewater via incomplete decomplexation by ozonation and subsequent resin adsorption. *Chemical Engineering Journal*, 435, 134923.
<https://doi.org/10.1016/j.cej.2022.134923>